Eur. Phys. J. Plus (2021) 136:735
https://doi.org/10.1140/epjp/s13360-021-01716-1

THE EUROPEAN
PHYSICAL JOURNAL PLUS

Regular Article

Spatial patterns in EEG activity during monotonous sound perception test

Anastasiya Runnova[1,2,a], **Maxim Zhuravlev**[1,2], **Rail Shamionov**[2], **Ruzanna Parsamyan**[1], **Evgeniy Egorov**[2], **Anton Kiselev**[1,3], **Anton Selskii**[2], **Olesya Akimova**[2], **Anatoly Karavaev**[1,2,4], **Jürgen Kurths**[2,5,6]

[1] Saratov State Medical University, B. Kazachaya Str., 112, Saratov, Russia 410012
[2] Saratov State University, Astrakhanskaya Str., 83, Saratov, Russia 410012
[3] National Medical Research Center for Therapy and Preventive Medicine, 10, Petroverigsky Per., Moscow, Russia 101953
[4] Saratov Branch of the Institute of RadioEngineering and Electronics of Russian Academy of Sciences, 38 Zelenaya Street, Saratov, Russia 410019
[5] Physics Department, Humboldt University, Newtonstrasse 15, 12489 Berlin, Germany
[6] Potsdam Institute for Climate Impact Research, Telegrafenberg A31, 14473 Potsdam, Germany

Received: 3 March 2021 / Accepted: 1 July 2021

Abstract We present a study of quantitative characteristics of a test subject attention associated with analysis of EEG-records in test subjects. Twelve overall healthy subjects 20–35 years old (5/7 male/female) with complaints about daytime sleepiness were included. Multichannel electroencephalography was conducted during the monotonous sound perception test. The processing of the EEG signals was based on the adapted method for assessing spatial patterns using the Karhunen–Loève transformation. We used descriptive statistics to summarize our findings. All experimental time was classified into active stages with reaction to sound stimuli and passive stages, in which subjects demonstrated drowsiness without reaction to presented stimuli. An analysis of EEG activity in conjunction with assessment of the patient response enabled us to identify a characteristic scenario of adaptation to the task of maintaining attention to sound stimuli in this group. Active stages with a minimum reaction time of response to the signal and maximum duration were preceded by an increase in the spatial activity complexity on the EEG of the left hemisphere during the passive stage without responses. The passive stage of drowsiness without response to stimuli was actively involved in the process of adaptation to prolonged monotonic activity in patients with increased daytime sleepiness.

1 Introduction

The surface electroencephalography (EEG) is widely used in studies of different physiological states of both humans and animals. The method of obtaining objective information about brain activity is convenient for investigators, as well as for study subjects, without specific complications imposed on conducting experimental work or clinical research. EEG,

[a] e-mail: a.e.runnova@gmail.com (corresponding author)

Published online: 09 July 2021

compared to other methods— e.g., magnetic resonance imaging (MRI), has disadvantages concerning deep spatial separation of brain activity zones. At the same time, high temporal resolution of EEG signals coming from the cerebral cortex surface is unattainable by other techniques. All objectives of the contemporary EEG data study are roughly divided into two major groups. The first group includes studying general patterns of brain activity accompanying different psychophysiological or neurological states of an animal, or a human—e.g., search for the markers associated with pathological activity preceding seizures [1,2], characteristic markers of the same type of cognitive processes in a person [3],or early precursors of developing the impairments in the cognitive or emotional domain [4]). The second group encompasses mathematical description of characteristic individual EEG patterns in a conditionally normal action and further automatic detection of such EEG patterns in brain–computer interface (BCI) systems [5–7]. As part of the latter, purely individual EEG patterns are habitually identified for every test subject or patient [8]. Moreover, such patterns frequently change with an increase in a subject's fatigue [9–11], or adapt when a subject's emotional state fluctuates [12]. Hence, artificial neural network (ANN) approaches are often used in the development of BCI systems [13–16].

At the same time, the contemporary methods of nonlinear dynamics are actively employed to detect and describe statistically significant EEG patterns. EEG dynamics is estimated using the methods of steady-state visually evoked potentials (SSVEP), or time–frequency domain detection based, for instance, on wavelet transformation. These methods allow giving both qualitative and quantitative assessment for oscillation energy of complex signals in different frequency ranges [17]. There is a number of techniques aimed at specific spatial definition of an EEG oscillation activity source, including independent component analysis (ICA) [18,19], empirical mode decomposition (EMD) [20], wavelet approaches for image denoising [21], etc. Identifying various parameter sets of spatial structures in EEG signals is yet another scope of this task, including estimation of the pattern duration and stability. The latter may be of interest for neurological diagnosing of pathological conditions [22,23] in terms of the changes in the brain activity in various psychological tests [24,25].

In this publication, we propose an adaptation of the conventional mathematical method based on the Karhunen-Loève decomposition (KL)—specifically, a proper orthogonal decomposition method (POD) for the analysis of spatiotemporal data [26]. This technique is extensively used to analyze the complex dynamics in various system types with both spatial and temporal degrees of freedom, for example, in hydrodynamics, plasma physics, and microwave optics [15,27]. Up to date, there were completed studies based on KL method for analyzing EEG data—in particular, an adaptation of the KL method was employed to compress EEG signals, while preserving spatial features [28], and an estimation of the spatial structure of the complexity in the brain electrical activity was proposed [29–31].

KL technique allows interpreting complex brain dynamics from the prospective of existence and interaction of coherent orthogonal space-time structures. Using experimental data as an example, we demonstrated an application of this method to investigating the changes in the EEG activity of test subjects with sleep disorder (daytime sleepiness). The characterization of this sleep disorder type is a daunting task for a sleep clinician, and such an assessment requires an in-depth medical history and, in many cases, objective evaluation in the sleep laboratory. An important and convenient practical tool for the clinical and scientific research of somnology issues is the Multiple Sleep Latency Test (MSLT) [32–34]. In our study, we used a specific variant of MSLT for conducting experimental recordings: the monotonous sound perception test. After that, we introduced the KL method for mathematical analysis of the EEG data in a group of overall healthy test subjects with complaints of daytime sleepiness.

As a result, we could identify changes in the brain activity of these subjects, correlating with improvement of a cognitive function of attention in our experiments.

2 Methods

2.1 Experimental design

Our experiments were conducted during the evening hours at a specially equipped laboratory, where every participating volunteer was in a comfortable semi-lying position; and effects of external stimuli, such as outside noise and bright light, were minimized. The experimental design is presented schematically in Fig. 1c). At the onset of the experiment, 6–7 minutes of EEG during passive wakefulness was recorded with participants' eyes closed. Then there were about 35 minutes of EEG recording during MSLT, followed by a repeated registration of the background condition with eyes closed for the same duration as in the beginning of the test.

During the active phase, every test subject was instructed to stay awake, largely with eyes open. To control the state of a subject, we employed pressing a button on a remote control, accompanied by beep sound. The sound signals were interspersed with pauses, the duration of which was set randomly in the range of (5; 11) s. The experimental work was attended

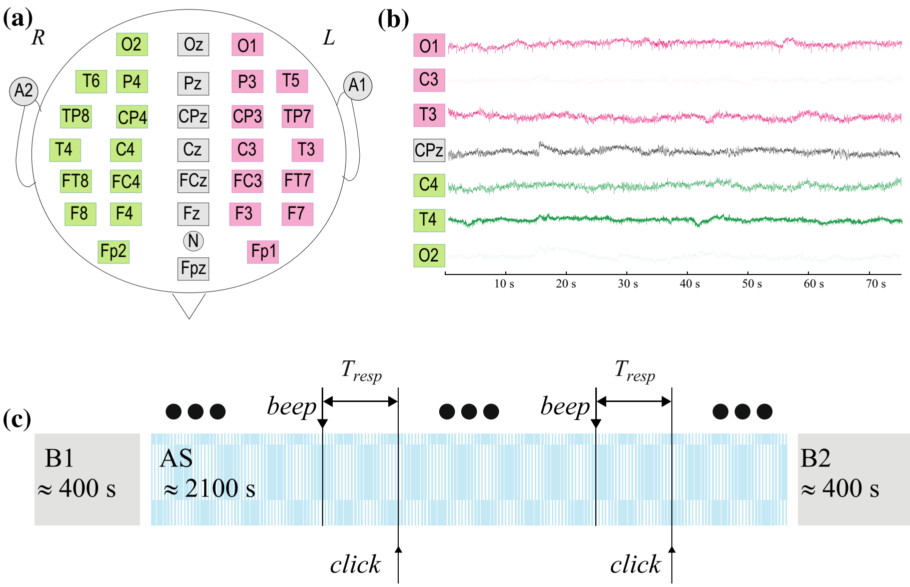

Fig. 1 **a** The scheme of the standard "10–10" EEG electrode arrangement. Different colors, pink and green, correspond to the scalp spatial zones of left and right hemispheres, Z_L and Z_R, respectively. **b** Fragments of EEG signals recorded during the experimental active stage. The signals are shown in colors in accordance with their association with the Z_L and Z_R zones. **c** The arrangement of the experiments: a light gray rectangle shows the first and last passive stages of the experiment (passive wakefulness with closed eyes), B1 and B2, respectively; a light blue rectangle with white patterns AS corresponds to the active stage; *beep*—time moments of sound stimuli; *click*—time moments of remote button pressing; ΔT_{resp}—the response time duration of a test subject for sound stimulus (*beep*). The total duration of active and passive stages is indicated on the respective rectangles. The number of *beeps* during the active stage was about 500

by 12 right-handed subjects 20–35 years old (5/7 male/female). The group of volunteers included overall healthy individuals with subjective complaints of daytime sleepiness. On the day before, and the day of the experimental work, none had an episode of a daytime sleep. The night sleep prior to the experiment was approximately 7 hr.

The exclusion criteria were as follows: (i) the sleep apnea/hypopnea syndrome; (ii) strong deviation from the age-specific norm of the cognitive status; and (iii) presence of emotional disorders. To identify disorders of cognitive and emotional status, anamneses for neurological disorders and neuropsychological testing were used, based on Montreal cognitive assessment (MoCA) [35] and Beck Depression Inventory [36].

During all experiments, the multichannel EEG data were obtained using the electroencephalographic recorder Encephalan-EEGR-19/26 (Medicom MTD, Russia). Data were recorded at 500 Hz sampling rate via the conventional monopolar registration method with two references and multiple electrodes ($N = 31$), as shown in Fig. 1a. The adhesive Ag/AgCl electrodes in special prewired headcaps were used to obtain EEG signals. Two reference electrodes, A1 and A2, were located on mastoids, while the ground electrode, N, was placed above the forehead. EEG signals were filtered by a bandpass filter with cutoff points at 0.5 Hz (HP) and 300 Hz (LP) and a 50 Hz notch filter. Fragments of EEG signals are presented in Fig. 1b.

All subjects participated in the experiment on a voluntary and gratuitous basis. They have signed an informed medical consent to participate in the experimental work, including their agreement for further publication of the results, and received all necessary explanations about the procedures. Collected experimental data were processed with respect to confidentiality and anonymity of research subjects.

2.2 Data analysis

To study spatial EEG dynamics, we used the method of assessing spatial modes of the Karhunen–Loève decomposition (KL). The orthogonal decomposition method *sensu* KL presumes solving an integral equation of the following form:

$$\int K(x, x^*)\Psi(x^*)\mathrm{d}x^* = \lambda\Psi(x), \tag{1}$$

where x is a spatial coordinate, t is the registration time, and $K(x, x^*)$ is the kernel of the equation, which can be presented as follows:

$$K(x, x^*) = \langle \xi(x, t)\xi(x^*, t)\rangle_t. \tag{2}$$

Here $\langle ...\rangle_t$ means time averaging. We can choose the space–time distribution of physical quantities as function $\xi(x, t)$. In this case, prior to creating the matrix of the kernel $K(x, x^*)$, it is necessary to set the value of $\xi(x, t)$ to zero mean.

Note that the KL decomposition is optimal, in sense that the eigenfunctions of Eqs. 1–2 form a basis such that the root-mean-squared error is minimized: $\epsilon = \min\langle\|\xi - \xi^N\|\rangle$, where ξ is the exact solution, ξ^N is approximate solution obtained for N basis dimension [37]. In this case, the solution of Eqs. (1)–(2) is reduced to finding a set of eigenvalues $\{\lambda_n\}$ and eigenvectors $\{\Psi_n\}$.

Each eigenvalue λ_n matches a specific eigenvector Ψ_n, determining the nth KL—mode of the oscillatory process. The value of λ_n is proportionate to the energy corresponding mode, which is convenient to consider in the normalized form:

$$W_n = \frac{\lambda_n}{\sum\limits_i \lambda_i} \times 100\%. \tag{3}$$

In our study, we choose time dependences of EEG recordings in different projection areas of the cerebral cortex as a function $\xi(x, t)$. The set (1)–(2) is a homogeneous Fredholm integral equation of the second kind (see [38]). To find eigenvectors and eigenvalues, it is necessary to represent the Eqs. (1)–(2) in a matrix form, and then the original equations can be rewritten as follows:

$$\sum_{p=1}^{n}\sum_{q=1}^{n} K(x_p, x_q)\Psi^k(x^q) = \sum_{p=1}^{n} \lambda_k \Psi^k(x^p), \quad k = \overline{1, n}, \tag{4}$$

$$K(x_p, x_q) = \frac{1}{T}\sum_{m=0}^{T} \left(\xi(x^p, t_m)\xi(x^q, t_m)\right), \tag{5}$$

where $\xi(x^p, t_m)$ and $\xi(x^q, t_m)$ are EEG signals, recorded from the scalp points x^p and x^q at time t_m; and T denotes the time interval of a recording.

The eigenvalues and eigenvectors of the matrix (5) can be found via the implicitly shifted QL-algorithm [39], after reducing the matrix $K(x_p, x_q)$ to a tridiagonal form by the Householder's method.

Mean, median, and standard deviation were used for the descriptive statistics of the data. The numerical computation of the KL transformation, along with statistical analysis, were conducted, using the original software developed in Fortran and Delphi systems.

3 Results

Let us consider the analysis of the behavioral characteristics of each tested subject's response to auditory stimuli. Figure 2a exhibits the smoothed dependence of the reaction time T_{resp} of the test subject #3 to the stimulus experimental duration time t. The computation of such smoothed T_{resp} dependence is based on estimating an average response time for each set of five consecutive sound signals pooled together. At the beginning and at the end of the experiment (areas on the graph, delineated by dotted lines), the subject rested without undertaking any action. For convenience, sequential numbering denotes the areas of different reactions of the subject to stimuli, whereas the numbers are not shown in the figure for narrow areas. At some points in time, the response time was dropping to zero (indicated in the figure by blue rectangles), which implied that no reaction to the stimulus from the subject was reported. These stages are interpreted as episodic sleeping of the subject.

As for behavioral characteristics, the entire duration of the experiment was divided into 17 stages. Stages B1 and B2 corresponded to the states of the test subject with eyes closed at the beginning and at the end of the experiment. We numbered the stages of the subject's active responses as A1–A8, where the number gradually increased in the course of the experiment, and the stages of conditional falling asleep as S1–S8 (Fig. 1c).

3.1 Karhunen–Loève modes

We estimated the values of the normalized energy W_n Eq. (3) of the first five KL modes ($N = 5$) for each of 17 stages of experimental work. The calculations were conducted for EEG signals recorded from the channels of the left and right spatial zones, Z_L and Z_R, highlighted by different colors in Fig, 1a. In Fig. 2, the panels (b) and (c) present the histograms of the normalized energy W_n distribution of the first five KL modes for each corresponding stage of our experimental work. The height of each histogram column corresponds to the

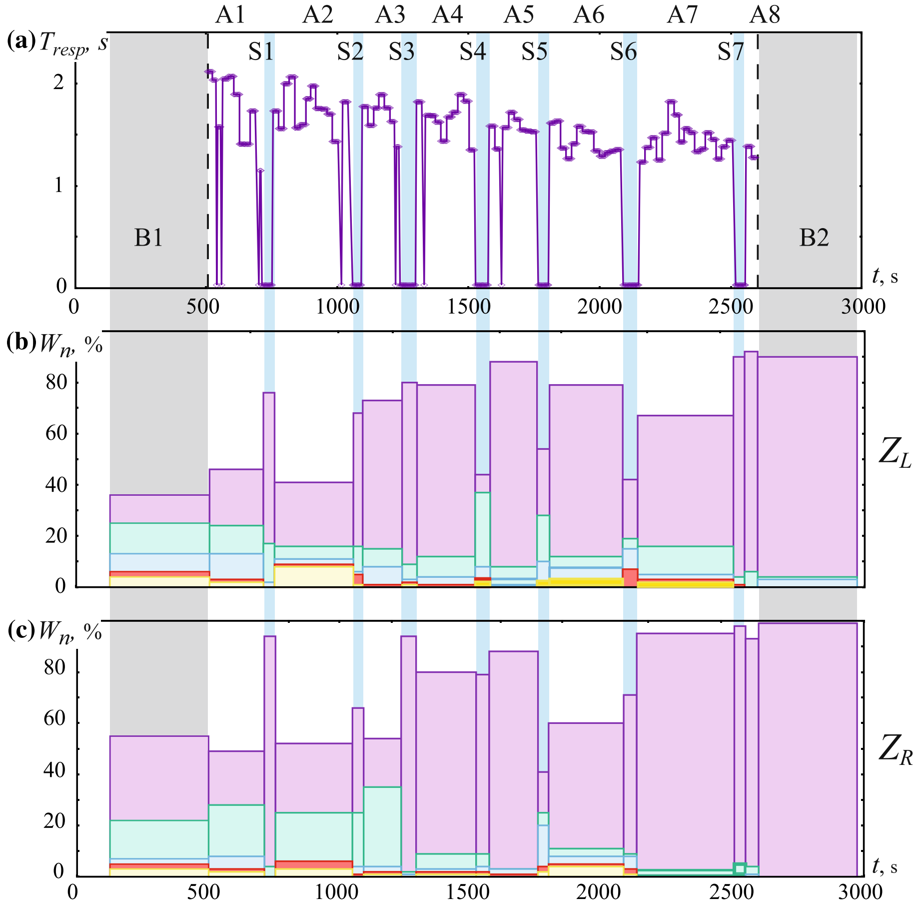

Fig. 2 Light gray rectangles indicate passive stages B1 and B2 with closed eyes of test subject. The active parts of the experiment was divided into 15 stages. **a** The dependence $T_{resp}(t)$ of the test subject's response duration to the sound stimulus during the experimental current time t. Vertical dashed lines indicate the beginning and end of the active experimental stage AS. The stages, at which the subject did not respond to sound stimuli, are shown in blue rectangles (S1 – S7). The experimental stages, at which the test subject actively responded to sound stimuli, are indicated as A1 – A8. **b**, **c** The distribution of the normalized energy W_n of the first five KL modes for experimental stages, for the left Z_L and right Z_R hemispheres, respectively. The height of the histogram column corresponds to the energy value of the certain KL mode, the color matches the mode number: mode 1—mauve, mode 2—green, mode 3— blue, mode 4—red, mode 5—yellow

energy of a particular mode, and the color matches the mode number. We assumed that KL modes with W_n amplitude exceeding 0.1 % of the largest mode amplitude were significant.

We discovered that the spatial EEG dynamics was significantly heterogeneous at various time intervals of the experiment. The number of significant modes for the regions under consideration varied from one to five. We estimated the number of $N_{KL}^{L,R}$ KL modes, characterizing the dynamics of each experimental stage for left and right hemispheres, Z_L and Z_R, respectively. In Fig. 3a, we demonstrate the dynamics of this parameter as a measure of the signal set complexity. In other words, the number of observed modes, when calculating the KL transformation, was increasing with the number of coherent patterns simultaneously developed in a given spatial zone of the brain projection, and also with complexity of the

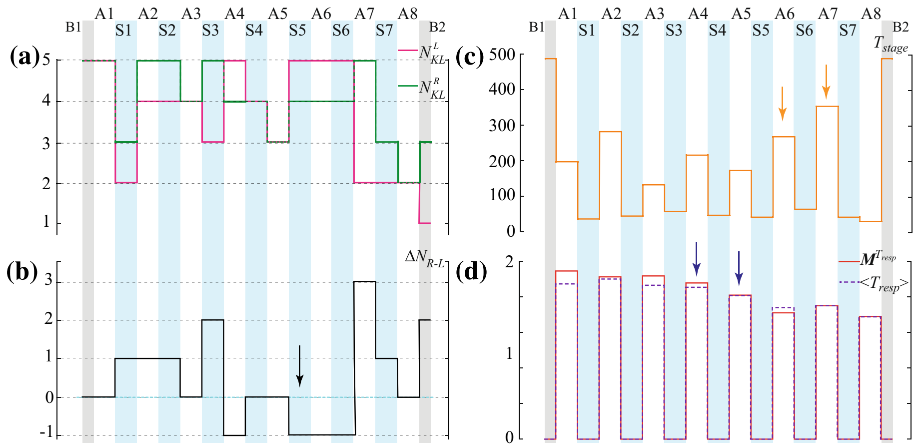

Fig. 3 Color and symbols denotations for various experimental stages in accordance with Figs. 1 and 2. **a** The number of $N^{L,R}_{KL}$ significant spatial KL modes for the left and right hemispheres zones Z_L (pink line) and Z_R (green line), calculated for different stages of experimental work; **b** the difference ΔN^{R-L} in the number of coherent spatial patterns for the zones Z_L and Z_R; **c** the duration of continuous stages identified in the experiment: B1, A1–A8, S1–S7, B2; **d** median $M^{T_{resp}}$ and the average $\langle T_{resp} \rangle$ reaction time of the subject, estimated for each experimental stage

EEG activity in this zone. To make the spatial dynamics comparison in the left vs. right hemispheres, we estimated the parameter: $\Delta N_{R-L} = N^R_{KL} - N^{L,R}_{KL}$ (Fig. 3b.

The structure of spatial activity in the right hemisphere demonstrated a large number N^R_{KL} of KL modes at seven stages of the experiment and, in addition, the average number $\langle N^R_{KL} \rangle = 4.13$. For the left hemisphere, the complexity of EEG activity increased just at four stages, and the average number $\langle N^L_{KL} \rangle \approx 3.69$.

During the first two stages (B1, A1) of the experiment, the activity in the Z_L and Z_R zones exhibited the maximum effort. After that, the spatial EEG dynamics of the Z_R zone increased the complexity, in comparison with the Z_L area, for the stages of episodic sleep up to A4, which is indicated by the arrow in Fig. 3b. Next, in the course of stages S4 and A5, the number of coherent patterns for the left and right hemisphere zones became the same, whereas during the stages S5, A6 and S6, the complexity of the spatial dynamics increased in Z_L. However, further on, the complexity of the structure in the left hemisphere declined to a minimum, and the spatial activity could be described by the KL modes 1 and 2.

For further analysis of the spatial EEG activity, we compared the EEG records with an independent assessment of a subject's response to sound stimuli. For each experimental stage, we calculated the duration T_{stage}, the median $M^{T_{resp}}$ and the average reaction time of a test subject response to the stimuli, $\langle T_{resp} \rangle$, as shown in Fig. 3c and d.

As for our results, there are several important points we would like to highlight: (**1**) We observed that duration of continuous wakefulness stages T_{stage} increased steadily after the stage A5, reaching a maximum at the stage A7 (351 s). Similarly, the duration of episodic sleep stages was not constant and varied from 46.239 s (stage S1) to 72.594 s (stage S6); (**2**) During the stage A5, the estimates of the mean and the median of a patient reaction time of response to the sound stimuli coincided, after reaction time demonstrated the minimum values until the end of the experiment ($M^{T_{resp}} = [1.367; 1.444; 1.3275]$, $\langle T_{resp} \rangle = [1.428; 1.448; 1.3275]$); (**3**) It is worth noting that stages A5 and A7 are characterized by virtually identical values

Table 1 Characteristics of EEG spatial activity and reaction time of the subjects: **#**—sequential number of test subject; **S#**—sequence number of stage S for which the condition $\Delta N_{R-L} < 0$ is satisfied; **A#**—sequence number of stage A for which the minimum of $M^{T_{resp}}$ is observed; **BAS**—the number of experimental stages for test subject #

#	S#, $\Delta N_{R-L} < 0$	A#, min $M^{T_{resp}}$	BAS	#	S#, $\Delta N_{R-L} < 0$	A#, min $M^{T_{resp}}$	BAS
1	8	10	19	7	3	6	9
2	3	4	7	8	12	13	17
3	5	6	17	9	5	6	9
4	4	6	10	10	4	6	9
5	8	6	18	11	6	7	10
6	–	–	3	12	5	7	18

of the median and the mean. Hence, for these stages, we can claim the subject reaction time distribution is approaching the normal distribution. However, this finding did not apply to stages A preceding the stage S5; (**4**) In subject #3, stage A8 was too short (39.661 s) to be included into the analysis.

Table 1 gives numerical summary of the spatial EEG patterns for a group of volunteers. For every test subject with a sequential number #, the sequential number of stage S is given, during which the spatial activity in the left Z_L zone demonstrated a large complexity in relation to the spatial activity in the right Z_R zone – i. e., $\Delta N_{R-L} < 0$; and the sequential number of stage A with the minimal reaction time of response, T_{resp}, of a volunteer is presented in the Table 1 as well. Additionally, we provide the full number of experimental stages for every test subject, BAS. It should be noted that subject #6 avoided episodes of a daytime sleep during the active phase of the experiment.

4 Conclusion

In our experiments, we observed changes in the structure of the EEG spatial activity in the hemispheres and simultaneous changes in quantitative characteristics of a test subject's attention, such as an ability to stay continuously awake (T_{stage}) and the reaction time of the patient's response to an auditory stimulus, T_{resp}. We discovered that a subject's reaction was becoming faster from the stage A4 on. Concurrently, the complexity of the left hemisphere spatial activity was growing as well. With an increase in the complexity of the left hemisphere activity during a short sleep (stages S5 and S6), we observed the minimal reaction time of a subject at the active stages A6 and A7, along with an increase in the duration of continuous wakefulness. The observed pattern was expressed in the sequential dynamics of the analyzed parameters: after a certain stage S with complications in the spatial activity of coherent patterns (KL modes), located in the left hemisphere zone, Z_L, the stage A emerged, which implied the minimal reaction time of response, distribution of the reaction time of response to stimuli close to normal, and increase in a continuous activity duration.

We investigated the repeatability of this scenario in the group of test subjects (Table 1). For 92% of those, we noticed a similarity in observed parameters of the spatial EEG activity and duration of reaction time of response to auditory stimuli. We assumed that an emergence of such spatial activity scenario was associated with the processes of brain activity optimization providing an increase in the efficiency of cognitive processes, which was expressed in a reduction in a reaction time of response, and an augmented duration of continuous stages of active wakefulness. The observed effect of the brain activity pattern resembled the detected scenarios of the spatial activity development shown in [24], in which higher speed and quality of a test solving procedure correlated with emergence of a more distributed functional network, forming solid connections within the nodes. We did not reveal any significant gender-related differences in the statistical analysis of observed EEG patterns and structures. However, the sample size was too small to exclude the possibility that a gender could constitute a lurking variable. Much larger sample would be required to prove otherwise in a further study.

Also, the high degree of homogeneity in the scenario of coherent spatial pattern development, observed in this study, could be, perhaps, associated with a presence of an essential feature in overall healthy volunteers—particularly, of a subjectively experienced excessive daytime sleepiness. High homogeneity of the group was established by the fact that 92% of test subjects demonstrated multiple stages of episodic daytime sleep without responses to stimuli. As shown in [25], subjects with similar psychological traits demonstrated similar electrical activity of the brain, recorded on their EEGs, in the course of taking complicated cognitive tests.

Cognitive activity parameters of subjects improved significantly after restructuring their brain activity during a sleep episode. For the group of 11 subjects with sleep stages S, the minimum values of the median $M^{T_{resp}}$ and the mean $\langle T_{resp} \rangle$ belonged to the ranges [1.1; 1.745] and [1.04; 1.75], respectively. However, the test subject #6 without episodic sleep stages had significantly smaller median and mean of reaction time of response to stimuli: $M^{T_{resp}} = 0.9$, $\langle T_{resp} \rangle = 0.89$. Indirectly, such increase in response times in a group of test subjects with daytime sleepiness may indicate an early stage of attention disorder—i.e., it is disguised for a subjectively perceived increase in a subject's daytime sleepiness. At the same time, absence of complaints for cognitive problems on the part of participants in the experimental group and the fact that such deviations were not exposed during a standard neuropsychological examination, present definite interest requiring further investigation.

Acknowledgements Obtaining neurophysiological data from volunteers as experimental part of this study was financed by the RF Government Grant No. 075-15-20191885. Adaptation of mathematical methods for data analysis in this project was carried out within the framework of the Government Procurement of the Russian Federation Ministry of Healthcare No. 056-00030-21-01 of May 02, 2021 Theoretical and Experimental Study of the Integrative Activity of Various Physiological Systems of Patient under Stress (the State registration number 121030900357-3). Russian Foundation for Basic Research (Grant No. 20-02-00752) supported the neurological analysis undertaken by R. Parsamyan.

Declarations

Conflict of interest The authors declare that they have no conflict of interest.

Ethical approval All procedures, performed in studies involving human participants, were in accordance with the 1964 Declaration of Helsinki and its later amendments or comparable ethical standards and approved by the local Research Ethics Committee of Saratov State Medical University.

Informed consent Informed consent was obtained from all individual participants involved in the study.

References

1. N.S. Frolov, V.V. Grubov, V.A. Maksimenko, A. Lüttjohann, V.V. Makarov, A.N. Pavlov, E. Sitnikova, A.N. Pisarchik, J. Kurths, A.E. Hramov, Statistical properties and predictability of extreme epileptic events. Sci. Rep. **9**(1), 1–8 (2019). https://doi.org/10.1038/s41598-019-43619-3
2. M. Lévesque, M. Avoli, High-frequency oscillations and focal seizures in epileptic rodents. Neurobiol. Disease **124**, 396–407 (2019). https://doi.org/10.1016/j.nbd.2018.12.016
3. A. Angelidis, M. Hagenaars, D. van Son, W. van der Does, P. Putman, Do not look away! Spontaneous frontal EEG theta/beta ratio as a marker for cognitive control over attention to mild and high threat. Biol. Psychol. **135**, 8–17 (2018). https://doi.org/10.1016/j.biopsycho.2018.03.002
4. W.J. Bosl, H. Tager-Flusberg, C.A. Nelson, EEG analytics for early detection of autism spectrum disorder: a data-driven approach. Sci. Rep. **8**(1), 1–20 (2018). https://doi.org/10.1038/s41598-018-24318-x
5. M.S. Bascil, A.Y. Tesneli, F. Temurtas, Spectral feature extraction of EEG signals and pattern recognition during mental tasks of 2-d cursor movements for BCI using SVM and ANN. Aus. Phys. Eng. Sci. Med. **39**(3), 665–676 (2016). https://doi.org/10.1007/s13246-016-0462-x
6. M.S. Bascil, A.Y. Tesneli, F. Temurtas, Spectral feature extraction of EEG signals and pattern recognition during mental tasks of 2-d cursor movements for BCI using SVM and ANN. Australasian physical & engineering sciences in medicine **39**(3), 665–676 (2016). https://doi.org/10.1007/s13246-016-0462-x
7. W. Zhang, C. Tan, F. Sun, H. Wu, B. Zhang, A review of EEG-based brain-computer interface systems design. Brain Sci. Adv. **4**(2), 156–167 (2018)
8. S. Saha, K.I.U. Ahmed, R. Mostafa, L. Hadjileontiadis, A. Khandoker, Evidence of variabilities in EEG dynamics during motor imagery-based multiclass brain-computer interface. IEEE Trans. Neural Syst. Rehabilit. Eng. **26**(2), 371–382 (2018). https://doi.org/10.1109/TNSRE.2017.2778178
9. F. Dehais, A. Dupres, G. Di Flumeri, K. Verdiere, G. Borghini, F. Babiloni, R. Roy, Monitoring pilot's cognitive fatigue with engagement features in simulated and actual flight conditions using an hybrid fNIRS-EEG passive BCI, in 2018 IEEE International Conference on Systems, Man, and Cybernetics (SMC), (IEEE, 2018), pp. 544–549. https://doi.org/10.1109/SMC.2018.00102
10. U. Talukdar, S.M. Hazarika, J.Q. Gan, Adaptation of common spatial patterns based on mental fatigue for motor-imagery BCI. Biomed. Signal Process. Control **58**, 101829 (2020). https://doi.org/10.1016/j.bspc.2019.101829
11. T. Zhang, T. Liu, F. Li, M. Li, D. Liu, R. Zhang, H. He, P. Li, J. Gong, C. Luo et al., Structural and functional correlates of motor imagery BCI performance: insights from the patterns of fronto-parietal attention network. Neuroimage **134**, 475–485 (2016). https://doi.org/10.1016/j.neuroimage.2016.04.030
12. D. Schubring, M. Kraus, C. Stolz, N. Weiler, D.A. Keim, H. Schupp, Virtual reality potentiates emotion and task effects of Alpha/Beta brain oscillations. Brain Sci. **10**(8), 537 (2020). https://doi.org/10.3390/brainsci10080537
13. S. Chaudhary, S. Taran, V. Bajaj, A. Sengur, Convolutional neural network based approach towards motor imagery tasks EEG signals classification. IEEE Sens. J. **19**(12), 4494–4500 (2019). https://doi.org/10.1109/JSEN.2019.2899645
14. K. Li, S. Ramkumar, J. Thimmiaraja, S. Diwakaran, Optimized artificial neural network based performance analysis of wheelchair movement for ALS patients. Art. Intell. Med. **102**, 101754 (2020). https://doi.org/10.1016/j.artmed.2019.101754
15. M. Hozic, A. Stefanovska, Karhunen-Loève decomposition of peripheral blood flow signal. Phys. A: Stat. Mech. App. **280**, 587–601 (2000). https://doi.org/10.1016/S0378-4371(00)00070-4
16. A.E. Hramov, A.A. Koronovskii, V.A. Makarov, A.N. Pavlov, E. Sitnikova, *Wavelets in Neuroscience* (Springer, 2015)
17. A.E. Hramov, A.A. Koronovskii, V.A. Makarov, A.N. Pavlov, E. Sitnikova, *Wavelets in Neuroscience* (Springer, Berlin, 2015)
18. K. Kobayashi, C. James, T. Nakahori, T. Akiyama, J. Gotman, Isolation of epileptiform discharges from unaveraged EEG by independent component analysis. Clin. Neurophysiol. **110**(10), 1755–1763 (1999). https://doi.org/10.1016/S1388-2457(99)00134-0
19. R. Labounek, D.A. Bridwell, R. Mareček, M. Lamoš, M. Mikl, T. Slavíček, P. Bednařík, J. Baštinec, P. Hluštík, M. Brázdil et al., Stable scalp EEG spatiospectral patterns across paradigms estimated by group ICA. Brain Topograph. **31**(1), 76–89 (2018). https://doi.org/10.1007/s10548-017-0585-8
20. A. Kybartaite, A. Kriščiukaitis, A. Gelžinis, A method for analysis of shape variation of visual evoked potentials based on Karhunen-Loève transform. Biomed. Eng. **17**(1), 50–54 (2013)
21. J.M. Lina, R. Chowdhury, E. Lemay, E. Kobayashi, C. Grova, Wavelet-based localization of oscillatory sources from magnetoencephalography data. IEEE Trans. Biomed. Eng. **61**(8), 2350–2364 (2012). https://doi.org/10.1109/TBME.2012.2189883

22. C. Babiloni, G.B. Frisoni, M. Pievani, F. Vecchio, R. Lizio, M. Buttiglione, C. Geroldi, C. Fracassi, F. Eusebi, R. Ferri et al., Hippocampal volume and cortical sources of EEG alpha rhythms in mild cognitive impairment and Alzheimer disease. Neuroimage **44**(1), 123–135 (2009). https://doi.org/10.1016/j.neuroimage.2008.08.005
23. A. Miao, J. Xiang, L. Tang, H. Ge, H. Liu, T. Wu, Q. Chen, Z. Hu, X. Lu, X. Wang, Using ictal high-frequency oscillations (80–500 Hz) to localize seizure onset zones in childhood absence epilepsy: a MEG study. Neurosci. lett. **566**, 21–26 (2014). https://doi.org/10.1016/j.neulet.2014.02.038
24. V.V. Makarov, M.O. Zhuravlev, A.E. Runnova, P. Protasov, V.A. Maksimenko, N.S. Frolov, A.N. Pisarchik, A.E. Hramov, Betweenness centrality in multiplex brain network during mental task evaluation. Phys. Rev. E **98**(6), 062413 (2018). https://doi.org/10.1103/PhysRevE.98.062413
25. V.A. Maksimenko, A.E. Runnova, M.O. Zhuravlev, P. Protasov, R. Kulanin, M.V. Khramova, A.N. Pisarchik, A.E. Hramov, Human personality reflects spatio-temporal and time-frequency EEG structure. PloS one **13**(9), 0197642 (2018). https://doi.org/10.1371/journal.pone.0197642
26. J.L. Lumley, The structure of ingomogeneous turbulent flows, in Atmospheric Turbulence and Radio Wave Propagation: Proc. of the Int. Colloquim, ed. by A.M. Yaglom, V.I. Tatarsky (Nauka, Moscow, 1967), p. 166
27. V.V. Makarov, M.O. Zhuravlev, A.E. Runnova, P. Protasov, V.A. Maksimenko, N.S. Frolov, A.N. Pisarchik, A.E. Hramov, Betweenness centrality in multiplex brain network during mental task evaluation. Physical Review E **98**(6), 062413 (2018). https://doi.org/10.1103/PhysRevE.98.062413
28. B. Hejrati, A. Fathi, F. Abdali-Mohammadi, Efficient lossless multi-channel EEG compression based on channel clustering. Biomed. Signal Process. Control **31**, 295–300 (2017). https://doi.org/10.1016/j.bspc.2016.08.024
29. K.A.I. Aboalayon, M. Faezipour, W.S. Almuhammadi, S. Moslehpour, Sleep stage classification using EEG signal analysis: a comprehensive survey and new investigation. Entropy **18**(9), 272 (2016). https://doi.org/10.3390/e18090272
30. W. Klonowski, W. Jernajczyk, K. Niedzielska, A. Rydz, R. Stepien, Quantitative measure of complexity of EEG signal dynamics. Acta Neurobiol. Exp. **59**(4), 315–321 (1999)
31. F. Pizza, L. Barateau, I. Jaussent, S. Vandi, E. Antelmi, E. Mignot, Y. Dauvilliers, G. Plazzi. Validation of multiple sleep latency test for the diagnosis of pediatric narcolepsy type 1. Neurology **93**(11), e1034–e1044 (2019). https://doi.org/10.1212/WNL.0000000000008094
32. M.A. Rahman, M.M. Haque, A. Anjum, M.N. Mollah, M. Ahmad, Classification of motor imagery events from prefrontal hemodynamics for BCI application, in Proceedings of International Joint Conference on Computational Intelligence (Springer, 2020), pp. 11–23. https://doi.org/10.1212/WNL.0000000000008094
33. M.R. Littner, C. Kushida, M. Wise, D.G. Davila, T. Morgenthaler, T. Lee-Chiong, M. Hirshkowitz, D.L. Loube, D. Bailey, R.B. Berry, S. Kapen, M. Kramer, Practice parameters for clinical use of the multiple sleep latency test and the maintenance of wakefulness test. Sleep **28**(1), 113–121 (2005). https://doi.org/10.1093/sleep/28.1.113
34. D. Schubring, M. Kraus, C. Stolz, N. Weiler, D.A. Keim, H. Schupp, Virtual reality potentiates emotion and task effects of Alpha/Beta brain oscillations. Brain Sciences **10**(8), 537 (2020). https://doi.org/10.3390/brainsci10080537
35. S. Freitas, M.R. Simoes, J. Marôco, L. Alves, I. Santana, Construct validity of the Montreal cognitive assessment (MoCA). J. Int. Neuropsychol. Soc. **18**(2), 242–250 (2012). https://doi.org/10.1017/S1355617711001573
36. D. Gallagher, G. Nies, L.W. Thompson, Reliability of the beck depression inventory with older adults. J. Consult. Clin. Psychol. **50**(1), 152 (1982). https://doi.org/10.1037/0022-006X.50.1.152
37. S. Watanabe, Karhunen-Loève expansion and factor analysis: theoretical remarks and application, in Trans. on 4th Prague Conf. Information Theory, Statistic Decision Functions, and Random Processes Prague (1965), pp. 635–660
38. T. Zhang, T. Liu, F. Li, M. Li, D. Liu, R. Zhang, H. He, P. Li, J. Gong, C. Luo et al., Structural and functional correlates of motor imagery BCI performance: Insights from the patterns of fronto-parietal attention network. Neuroimage **134**, 475–485 (2016). https://doi.org/10.1016/j.neuroimage.2016.04.030
39. F. Acton, *Numerical Methods That Work, Corrected*, Edition edn. (Mathematical Association of America, Washington, 1990)